AAPS PharmSciTech, Vol. 13, No. 2, June 2012 (© 2012)
DOI: 10.1208/s12249-012-9789-0

Research Article

Structure and Dissolution of L-Leucine-Coated Salbutamol Sulphate Aerosol Particles

Janne Raula,[1,4] Jukka Seppälä,[2] Jari Malm,[3] Maarit Karppinen,[3] and Esko I. Kauppinen[1]

Received 25 January 2012; accepted 4 April 2012; published online 5 May 2012

Abstract. L-Leucine formed different crystalline coatings on salbutamol sulphate aerosol particles depending on the saturation conditions of L-leucine. The work emphasizes a careful characterization of powders where structural compartments such as crystal size and particle coating may affect the performance of drug when administered. The sublimation of L-leucine from the aerosol particles took place 90°C lower temperature than the bulk L-leucine which was attributed to result from the sublimation of L-leucine from nano-sized crystalline domains. The dissolution slowed down and initial dissolution rate decreased with increasing L-leucine content. Decreasing crystalline domains to nano-scale improve heat and mass transfer which was observed as the lowered decomposition temperature of the drug salbutamol sulphate and the sublimation temperature of surface material L-leucine as well as the altered dissolution characteristics of the drug. The structure of the coated drug particles was studied by means of thermal analysis techniques (DSC and TG), and the dissolution of salbutamol sulphate was studied as an on-line measurement in a diffusion cell.

KEY WORDS: aerosol; dissolution; L-leucine coating; nanocrystals; sublimation.

INTRODUCTION

In drug delivery systems, any changes in particle properties may affect dosing and possibly the bioavailability of drug when administered to a patient. For instance, the dissolution of amorphous drug is preferably faster than that of crystalline counterpart (1,2). Amorphous drug particles may also crystallize upon storage resulting in undesired characteristics such as strongly agglomerated particles or altered polymorphism. Moreover, it has been shown that downsizing materials from bulky to nano-scale objects has been shown to alter physical properties to result in, *e.g.* decreased melting temperature (3–6) and improved material solubility (7–9). Many particle features including drug crystallinity (10), particle morphology (11) and internal structure (12) may notably vary according to the technology used. In medicine, any unexpected features in drug formulations may lead to drastic changes in drug pharmacokinetics (*e.g.* particle delivery and uptake by cells) and pharmacodynamics (*e.g.* solubility due to high surface-to-volume ratio). Therefore, a control over particle formation and careful characterization of the formulation are essential in order to evaluate material behaviour in specific applications.

We recently reported the preparation of salbutamol sulphate particles coated with amino acid L-leucine in an aerosol flow reactor (12–15). At fixed saturation conditions, L-leucine formed a crystalline encapsulating layer by molecular diffusion to the droplet surface or a crystalline, rough nano-sized coating layer by physical vapour deposition (PVD) or both of the layers at particle surface. Both layers were crystalline (16). The rough coating layer provided excellent powder aerosolization (17), whereas the encapsulating layer protected the particles against moisture (18).

The work emphasizes demonstrating the effect of different structures in powder assemblies and crystallinities on the thermodynamics of materials and the dissolution performance of salbutamol sulphate. The structure of the coated drug particles was studied by means of thermal analysis techniques (differential scanning calorimetry (DSC) and thermogravimetric (TG)), and the dissolution of salbutamol sulphate was studied as an on-line measurement in a diffusion cell.

MATERIALS AND METHODS

Materials

Salbutamol sulphate, *S*(bulk) (Alfa Aesar, Germany) and L-leucine, *L*(bulk) (Fluka, Switzerland) were used as received. Micronized salbutamol sulphate powder S(micr) was received as a gift from Gamprex (Italy). Precursor solutions for pure salbutamol sulphate and L-leucine particles and for composite particles were made, respectively, by the separate dissolution and co-dissolution of salbutamol sulphate (30 g/l) and L-leucine (2.5 and 15 g/l) in deionized water.

Electronic supplementary material The online version of this article (doi:10.1208/s12249-012-9789-0) contains supplementary material, which is available to authorized users.

[1] Department of Applied Physics, Aalto University School of Science, P.O. Box 15100, FI-00076 AALTO, Espoo, Finland.
[2] Department of Biotechnology and Chemical Technology, Aalto University School of Chemical Technology, P.O. Box 16000, FI-00076 AALTO, Espoo, Finland.
[3] Department of Chemistry, Aalto University School of Chemical Technology, PO Box 16100, FI-00076 AALTO, Espoo, Finland.
[4] To whom correspondence should be addressed. (e-mail: janne.raula@aalto.fi)

Table I. Experimental Conditions for the Production of Fine Powders from the Precursor Solutions and Some Characteristics of the Powder

	Preparation				Produced powder				
Sample	*S* (wt%)	*L* (wt%)	*T* (°C)	Surface	*S* (wt%)[a]	*L* (wt%)[b]	*n*(*L*)[b]	GNMD (μm)	GSD
S96L04-100	92	8	100	E	96	4	0.07	1.1	2.6
S82L18-100	67	33	100	E	82	18	0.29	1.2	2.8
S97L03-160	92	8	160	E+C	97	3	0.05	n.a.	n.a.
S82L18-160	67	33	160	E+C	82	18	0.29	n.a.	n.a.

S salbutamol sulphate, *L* L-leucine, *T* reactor temperature, *GNMD* geometric number mean diameter, *GSD* geometric standard deviation, *E* the particles encapsulated by L-leucine by surface diffusion, *C* the particles coated by the PVD of L-leucine
The size distribution were not applicable (n.a.) for the samples S97L03-160 and S82L18-160 due to the overlapping of the distributions of the pure L-leucine particles formed *via* homogeneous nucleation and the coated drug particles formed *via* heterogeneous nucleation by L-leucine vapour
[a] ^{1}H-NMR in D_2O
[b] Molar fraction of L-leucine in the powder

Particle Production

Particle preparation by the aerosol flow reactor has been discussed in detail in our previous work (12, 18). Briefly, the solute droplets formed from the precursor solutions (ultrasonic nebulizer RBI Pyrosol 7901) containing salbutamol sulphate and L-leucine were dried to form solid microparticles in the gas phase. The droplets were transferred with nitrogen gas (10 l/min) to the stainless steel aerosol reactor where temperatures were 100 and 160°C (±1°C). At the reactor downstream, the aerosol was rapidly diluted and cooled with a large volume of N_2 gas (22°C, 80 l/min; Reynolds number >3,000) in a porous stainless steel tube to avoid the wall deposition of particles and to initiate the nucleation and deposition of L-leucine vapour on drug particle surfaces. The solid aerosol particles were collected by a small-scale cyclone (19).

Characterization

The number size distributions of the produced particles were determined with an electrical low-pressure impactor (Dekati Ltd., Finland). Oiled porous collection substrates with stage aerodynamic cutoff diameters from 0.03 to 7.88 μm were used to avoid particle bounce. The density of the particles was approximated to be 1 g/cm^3.

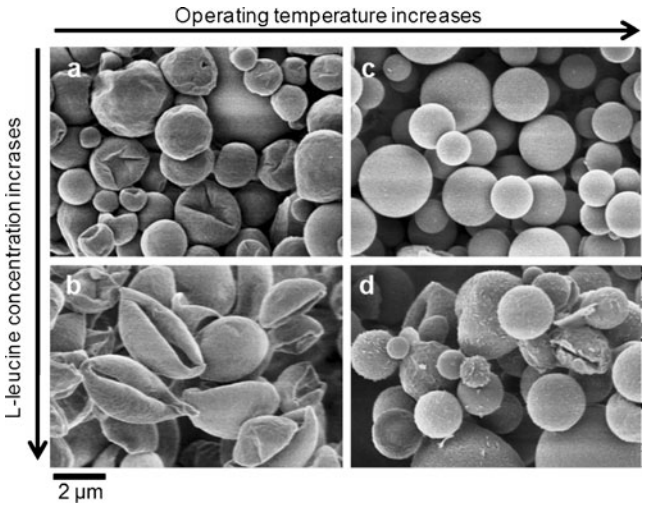

Fig. 1. SEM images of the L-leucine coated salbutamol sulphate particles prepared at 100°C **a** S96L04-100, **b** S82L18-100, and prepared at 160°C **c** S97L03-160, **d** S82L18-160

The morphology of the particles was imaged with field-emission scanning electron microscopy, SEM (Leo DSM982 Gemini) at an acceleration voltage of 2 kV. The samples were coated with sputtered platinum in order to stabilize them under the electron beam and to enhance image contrast.

The powder compositions were determined by nuclear magnetic resonance spectrometry, NMR (200 MHz, Varian Gemini 2000). Deuterated water was used as a solvent. The characteristic chemical shifts used were 6.8–7.4 ppm (3H, phenyl protons) for salbutamol sulphate and 0.8–1.0 ppm (6H, methyl protons) for L-leucine.

The particle crystallinity before humidification was analysed by X-ray diffraction (XRD) using a powder diffractometer (control unit Philips PW 1710, goniometer Philips PW 1820, generator Philips PW 1830, The Netherlands) and CuKα radiation (40 kV, 50 mA, with wavelengths $K\alpha_1$ of 0.154060 nm and $K\alpha_2$ of 0.154439 nm, with an α_1/α_2 intensity ratio of 0.5). The XRD patterns were recorded at 2θ angles from 3° to 40° using a step size of 0.02° and a scan speed of 0.004°/s.

Calorimetric measurements were conducted using differential scanning calorimetry, DSC (Mettler Toledo DSC 821) in a gaseous nitrogen atmosphere. The samples were heated from 25 to 250°C with a heating rate of 10°C/min.

TG measurements were carried out using a Netzsch STA 449C (Netzsch-Gerätebau GmbH, Germany) thermobalance. The samples weighing 5 to 15 mg were heated from 25 to 270°C with a heating rate of 10°C/min under dynamic nitrogen atmosphere with a flow rate of 40 ml/min.

Dissolution studies were conducted in an in-house-made diffusion cell cuvette (pH 7.4, 37°C) following the absorption of salbutamol (λ_{set} 278 nm) on-line at 1-s intervals as a function of time (UV/Vis spectrometer, Perkin Elmer, Lambda 950). The diffusion membrane was regenerated cellulose with MWCO 6–8 kDa (ZelluTrans, Roth). The pH of the buffer solution was adjusted to pH 7.4 with NaOH (1.6 g/l) and KH_2PO_4 (6.8 g/l) in Milli-Q water. For the study, the powder sample (100–200 mg) was placed on top of the membrane of the diffusion cell cuvette filled with the buffer solution (the cuvette was tempered at 37°C). Then 0.2 ml of the buffer (37°C) was placed on the sample which was used as an onset for recording absorption. The dissolution was calculated by Abs(measured)/Abs(loaded)×100%. Initial dissolution rates were determined by the dissolved moles of drug as functions of time and the permeation area of the membrane. The calibration was conducted at the concentration range of 0.01–0.1 g/l in Milli-Q water. See ESM Figure S1 for the schematics of the dissolution cell.

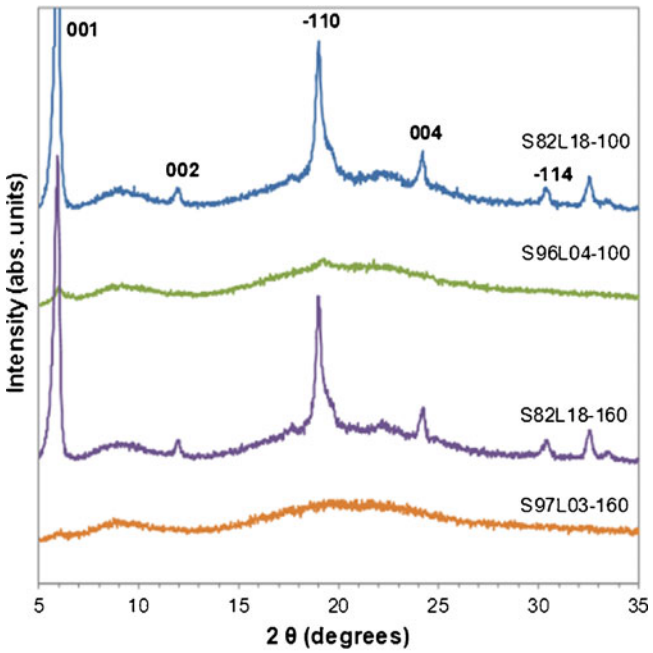

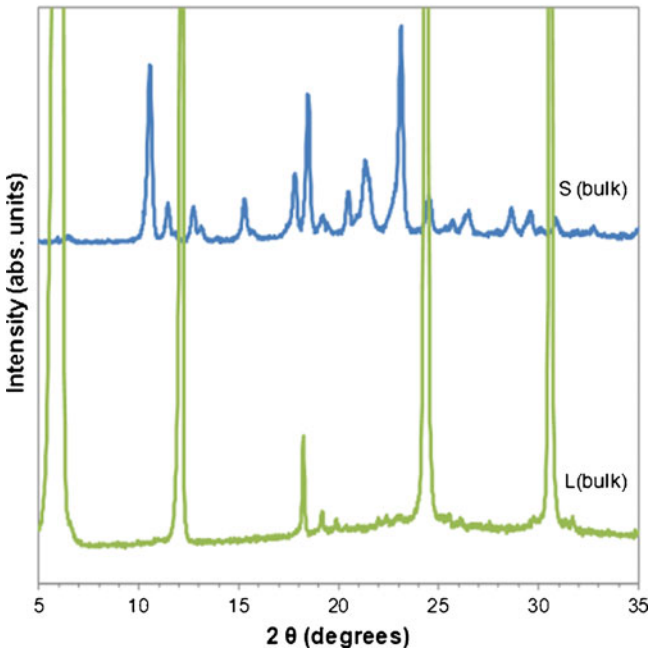

Fig. 2. XRD patterns of the samples. The diffraction peaks (*001*), (*002*), (*−110*), (*004*) and (*−114*) of L-leucine are marked in the figure

RESULTS AND DISCUSSION

Particle Morphology

Table I reviews the experimental set-up of particle preparation and the characteristics of the powders, and Fig. 1 shows particle morphologies. In consistent with the previous results (16,18), in this study the morphology of particles depended on the saturation conditions of L-leucine as follows, see Fig. 1. At reactor temperature 100°C where L-leucine was fully in a saturated state (Fig. 1a, b), surface-active L-leucine formed an encapsulating surface layer by molecular accumulation on a gas-droplet interface prior to particle drying

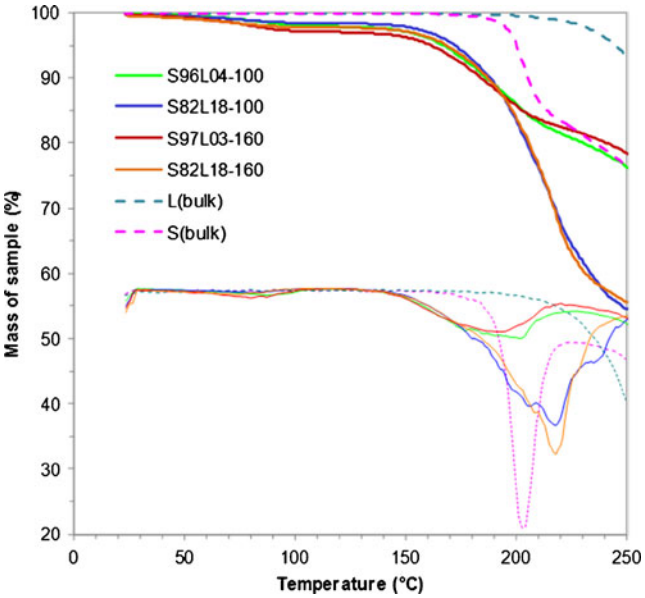

Fig. 3. TG thermograms of the samples. The *insets* show the derivatives of the TG thermograms

resulting in wrinkled particle morphology became with the addition of L-leucine. At reactor temperature 160°C where

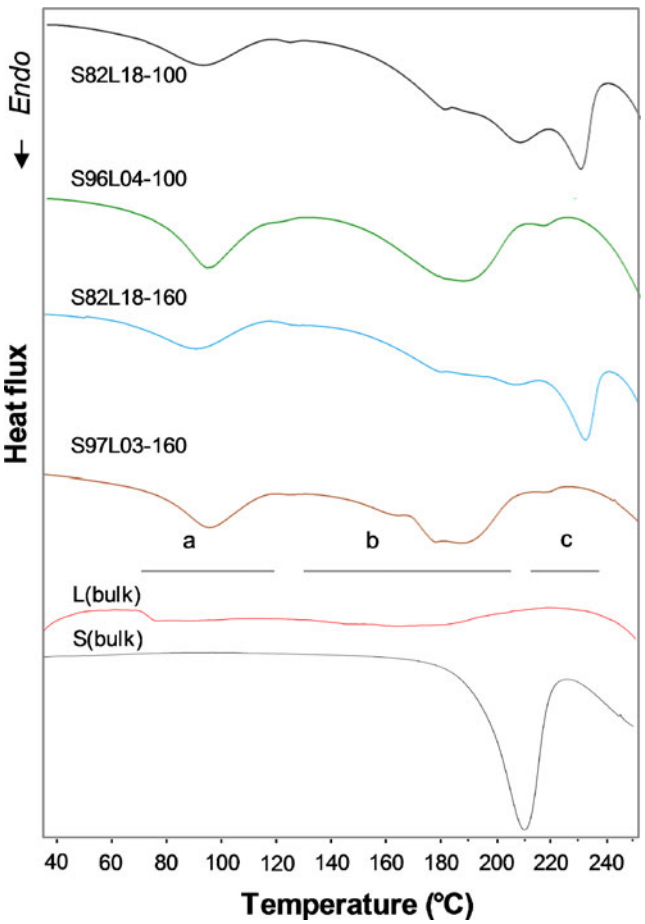

Fig. 4. DSC thermograms of the samples. The regions of thermal transitions are **a** 50–115°C is for the evaporation of residual water, **b** 130–205°C for the melting of salbutamol sulphate crystals, **c** 200–235°C for the sublimation of L-leucine

Table II. Characteristics of the Samples Measured by Differential Scanning Calorimetry and Thermogravimetry

	50–115°C				130–200°C	190–235°C			
	T_{peak} °C	−ΔH J/g	Content %		−ΔH J/g	T_{peak} °C (T_{onset})	−ΔH J/g	wt% (T range)	T_{peak} °C
Sample	DSC	DSC	DSC[a]	TG	DSC	DSC	DSC	TG	TG
S96L04-100	91	34	1.5	2.1	73	212 (206)	2.2	1.0 (205–218)[b]	200
S82L18-100	89	26	1.1	1.6	45	225 (217)	32.9	14.5 (213–234)[b]	216
S97L03-160	92	39	1.7	3.0	78	214 (208)	1.8	1.0 (207–220)[b]	191
S82L18-160	88	36	1.6	2.3	40	227 (215)	36.7	15.5 (212–235)[b]	217

T_{peak} peak temperature, T_{onset} onset temperature
[a] Estimated by the relation to the heat of water evaporation at 373.15 K as 2,257 J/g
[b] The contribution of the decomposition of salbutamol sulphate to mass loss within the studied temperature range has been subtracted

L-leucine was partially in a vapour phase (Fig. 1c, d), L-leucine formed the coating layer by physical vapour deposition on the drug particle surfaces upon cooling. Upon the deposition, L-leucine formed small crystals pointing outwards from the particle surface. As a consequence in the latter case, the salbutamol sulphate particles contained two L-leucine outer layers that were the encapsulating and coating layers. It should be noted, however, that the particles with the 3 wt% of L-leucine (S97L03-160) may contain merely the coating layer formed *via* vapour deposition due to the lack of wrinkled morphology typical for the encapsulated particles.

XRD Studies

The formation and crystallinity of L-leucine nanoparticles prepared in the aerosol reactor at varying saturation conditions have been studied in our previous work (Raula *et al.* 2007). These nanoparticles were crystalline regardless of the saturation conditions of L-leucine. The characteristic diffraction peaks of salbutamol sulphate were not present in the studied particles indicating that salbutamol sulphate was amorphous, see Fig. 2. However, the characteristic crystalline peaks for L-leucine appeared and increased as its content increased. The crystallization of L-leucine in the both ways of particle formation preferred the (−110) direction over the (001) direction as the (−110) peak was much stronger in the present samples compared with the case of bulky L-leucine crystals. The intensity ratio (001)/(−110) in bulk L-leucine was 340 whereas the (−110) orientation became notably pronounced as the content of L-leucine increased in the aerosol particles. The ratios of (001)/(−110) for S96L04-100, S82L18-100 and S82L18-160 were 1.3, 2.1 and 2.3. This ratio for S97L03-160 could not be determined.

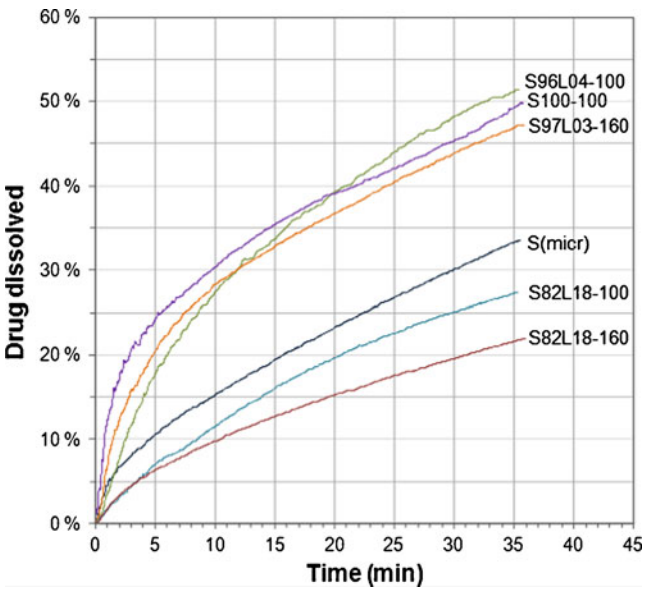

Fig. 5. Dissolution of salbutamol sulphate from the particles as a function of time in the diffusion cell cuvette. The UV absorption was recorded at λ=278 nm. The curves are the averages of two measurements

Thermoanalytical Studies

Figures 3 and 4 show the thermograms and Table II summarizes the main results of the DSC and TG measurements. The melting of bulk salbutamol sulphate crystals took place approximately 202°C which was observed as an endotherm (DSC) and partial mass loss which is due to decomposition. Amorphous salbutamol sulphate in the aerosol particles showed the mass loss starting at approximately 140°C and the endotherms within 130–205°C attributed to salbutamol decomposition. The overall mass loss increased upon heating as the content of L-leucine increased. The derivatives of the TG curves showed that the mass loss was the most intense within 191–217°C (see the derivative minima in the insets of Fig. 3). The latter samples also showed additional endotherms in DSC within 200–235°C whose enthalpies and onset temperatures increased with added L-leucine which was attributed to result from the sublimation of L-leucine, see Fig. 4. The contribution of L-leucine sublimation on the mass loss at this temperature range was assumed to be substantial to the decomposition of salbutamol due to the elevated peak temperatures. The increase in enthalpy and mass loss can be understood by the increased amount of L-leucine to sublime. However, the lowered sublimation temperature of L-leucine and the decrease in the onset temperature with added L-leucine could be explained by the crystal size of L-leucine: the low sublimation temperature, which was substantially lower than that of bulky L-leucine (~295°C (20)), and its raise are expected to be caused by nano-sized crystals whose size increased as the amount of L-leucine increased. As the crystal size would reach the size of bulk L-leucine crystals, the sublimation initiates approximately 200°C, see Fig. 3. Based on the result that the bulk L-leucine samples did not show endotherms at 200–235°C but slight endothermic decreases above

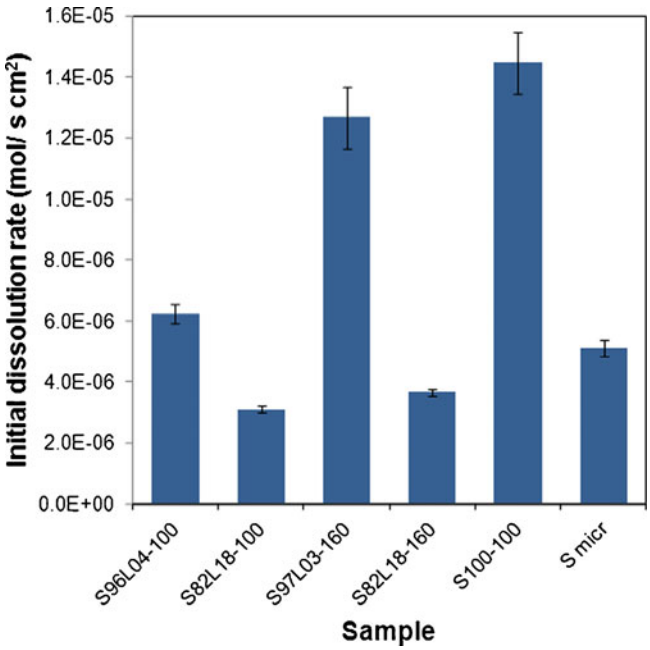

Fig. 6. Initial dissolution rates of salbutamol sulphate calculated from the slope of the tangent at the onset of dissolution

230°C, it can be concluded that the crystalline domains of L-leucine in the salbutamol sulphate particles are distinctively smaller than in the bulk L-leucine. Accordingly, the thermal behaviour of the aerosol samples can be divided roughly in following sections: the removal of residual water at 50–115°C, the decomposition of salbutamol sulphate from 140°C upwards, and the sublimation of L-leucine nanocrystals at 205–235°C.

Dissolution Studies

Figure 5 shows the dissolution of salbutamol sulphate from the aerosol particles which are compared to the relevant reference powder, crystalline micronized salbutamol sulphate. Salbutamol sulphate dissolved from the pure, mainly amorphous salbutamol sulphate spherical particles S100-100 (geometric number mean diameter (GNMD) 1.1 μm) prepared at 100°C (18) and from the two powders with the lowest L-leucine faster than from the micronized particles within the first 10 min, after that the dissolution rates were approximately the same through the membrane. The faster dissolution from the aerosol particles is explained by the amorphous salbutamol sulphate that is more accessible to solvent than crystalline material thus promoting enhanced dissolution. The slowed dissolution with added L-leucine is explained by the solubility difference: L-leucine is less soluble in water (approximately 24 g/l) than salbutamol sulphate which is freely soluble. Thus, the coating layer of L-leucine slowed down the dissolution of salbutamol sulphate which was particularly observed in the beginning the dissolution. Also, the surfaces of S96L04-160 and S97L03-160 particles were not fully covered with L-leucine based on a calculation where a complete particle surface coverage by L-leucine for the 1.0 μm spherical particle is reached with 8.65×10^{6} L-leucine molecules that corresponds the L-leucine concentration of 3.6 g/l in the precursor solution (the cross-sectional area of the L-leucine molecule is 0.36 nm^2 (21)). However, at high L-leucine concentration, the surface is fully covered by L-leucine which slowed down the dissolution of salbutamol sulphate. This hindered dissolution of the drug is justified by the lower solubility of L-leucine than salbutamol sulphate as discussed above. The initial dissolution rates were calculated from the slope of the tangent from the onset of dissolution, see Fig. 6. The fastest initial dissolution was performed by S100-100. The rates decreased with increasing L-leucine content in the samples but this was more pronounced in the samples prepared at 160°C (8.1×10^{-6} mol/s cm^2 (L-leucine 3 wt%)–2.4×10^{-6} mol/s cm^2 (L-leucine 18 wt%)) than in the samples prepared at 100°C (4.0×10^{-6} mol/s cm^2 (L-leucine 4 wt%) – 2.0×10^{-6} mol/s cm^2 (L-leucine 18 wt%)). The difference between the particle sets is assumed to arise from smaller crystal domains of L-leucine in the coating layer of the powders prepared at 160°C than in the encapsulating layer of the powders prepared at 100°C due to the lower L-leucine concentration in vapour than as accumulated at the droplet/particle surface.

CONCLUSIONS

We have shown that the preparation and saturation conditions affect the resulting structural characteristics of particles. The results discussed above indicate that the studied particles are composed of amorphous salbutamol sulphate particle core encapsulated and coated with nano-sized L-leucine crystals. Figure 7 illustrates schematically the particle structure for the

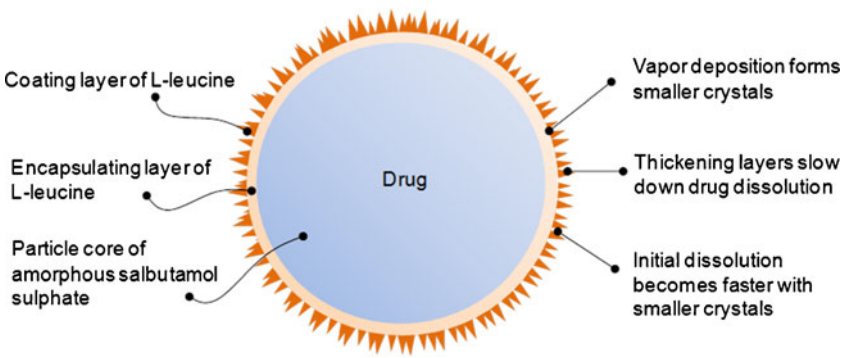

Fig. 7. Scheme of the structure of the aerosol particles of salbutamol sulphate core encapsulated and coated with L-leucine

aerosol particles with the both encapsulating and vapour-deposited layers of L-leucine and summarizes the main features that showed to affect drug dissolution. A careful characterization is vital to estimate the drug performance such as dissolution and bioavailability when delivered to a patient. As demonstrated in this work, decreasing crystalline domains to nano-scale may improve heat and mass transfer which was observed as the lowered decomposition temperature of the drug salbutamol sulphate and the sublimation temperature of surface material L-leucine as well as the altered dissolution characteristics of the drug. Accordingly, a careful selection of preparation conditions to manipulate material characteristics in drug powders can be beneficial for controlling drug performance.

ACKNOWLEDGMENTS

We thank Academy of Finland (project nos. 133407 and 140362) for financial support.

REFERENCES

1. Hancock BC, Zografi G. Characteristics and significance of the amorphous state in pharmaceutical systems. J Pharm Sci. 1997;86:1–12. and references therein.
2. Hancock B, Zografi G. The relationship between the glass transition temperature and the water content of amorphous pharmaceutical solids. Pharm Res. 2008;11:471–7.
3. Dick K, Dhanasekaran T, Zhang Z, Meisel D. Size-dependent melting of silica-encapsulated gold nanoparticles. J Am Chem Soc. 2002;124:2312–7.
4. Lai SL, Guo JY, Petrova V, Ramanath G, Allen LH. Size-dependent melting properties of small tin particles: nanocalorimetric measurements. Phys Rev Lett. 1996;77:99–102.
5. Jiang Q, Shi HX, Zhao M. Melting thermodynamics of organic nanocrystals. J Chem Phys. 1999;111:2176–80.
6. Jiang Q, Zhang Z, Li JC. Melting thermodynamics of nanocrystals embedded in a matrix. Acta mater. 2000;48:4791–5.
7. Chingunpituk J. Nanosuspension technology for drug delivery. Walailak J Sci Technol. 2007;4:139–53.
8. Liu P, Rong X, Laruc J, van Veen B, Kiesvaara J, Hirvonen J, Laaksonen T, Peltonen L. Nanosuspensions of poorly soluble drugs: preparation and development by wet milling. Int J Pharm. 2011;411:215–22.
9. Laaksonen T, Liu P, Rahikkala A, Peltonen L, Kauppinen EI, Hirvonen J, Järvinen K, Raula J. Intact nanoparticulate indomethacin in fast dissolving carrier particles by combined wet milling and aerosol flow reactor methods. Pharm Res. 2011; 28:2403–11.
10. Ward GH, Schultz RK. Process-induced crystallinity changes in albuterol sulfate and its effect on powder physical stability. Pharm Res. 1995;12:773–9.
11. Chew NYK, Chan H-K. Use of solid corrugated particles to enhance powder aerosol performance. Pharm Res. 2001;18:1570–7.
12. Raula J, Kuivanen A, Lähde A, Kauppinen EI. Gas-phase synthesis of L-leucine-coated micrometer-sized salbutamol sulphate and sodium chloride particles. Powder Technol. 2008;187:289–97.
13. Lähde A, Raula J, Kauppinen EI. Simultaneous synthesis and coating of salbutamol sulphate nanoparticles with L-leucine in the gas phase. Int J Pharm. 2008;358:256–62.
14. Lähde A, Raula J, Kauppinen EI. Combined synthesis and *in-situ* coating of nanoparticles in the gas phase. J Nanoparticle Res. 2008;10:121–30.
15. Raula J, Lähde A, Kauppinen EI. A novel gas phase method for the combined synthesis and coating of pharmaceutical particles. Pharm Res. 2008;25:242–5.
16. Raula J, Kuivanen A, Lähde A, Jiang H, Antopolsky M, Kansikas J, Kauppinen EI. Synthesis of L-leucine nanoparticles via physical vapor deposition under various saturation conditions. J Aerosol Sci. 2007;38:1172–84.
17. Raula J, Lähde A, Kauppinen EI. Aerosolization behavior of carrier-free L-leucine coated salbutamol sulphate powders. Int J Pharm. 2009;365:18–25.
18. Raula J, Thielmann F, Kansikas J, Hietala S, Annala M, Seppälä J, Lähde A, Kauppinen EI. Investigations on the humidity-induced transformations of salbutamol sulphate particles coated with L-leucine. Pharm Res. 2008;25:2250–61.
19. Zhu Y, Lee KW. Experimental study on small cyclones operating at high flow rates. J Aerosol Sci. 1999;30:1303–15.
20. Li J, Wang Z, Yanga X, Hua L, Liu Y, Wang C. Decomposing or subliming? An investigation of thermal behavior of L-leucine. Thermochim Acta. 2006;447:147–53.
21. Hasegawa K, Miyashita S, Komatsu H, Sano C, Nagashima N. *In-situ* observation of the concentration gradient layer around a growing crystal of leucine complex. J Crystal Growth. 1996; 166:925–9.